Experimental investigation of suspended load deposition on paddy fields during fluvial inundation

Can DING[1], Kenji KAWAIKE[2], Hajime NAKAGAWA[2] and Kazuki YAMANOI[2]

Experimental investigation of suspended load deposition
on paddy fields during fluvial inundation

Can DING[1], Kenji KAWAIKE[2], Hajime NAKAGAWA[2]
and Kazuki YAMANOI[2]

Abstract

In this study, physical experiments were performed to investigate the influence of two key morphological factors in paddy fields, i.e., paddy ridges and irrigation channels, on sediment deposition during fluvial inundation. The inlet boundary was given constant water and sediment discharges to simulate embankment failure conditions. Hydraulic parameters show that sediment came into the floodplain in the form of suspended load. By changing the outlet boundary and channel outlets conditions, three groups of experiments were conducted. The results show that, under the high-water-level scenario (with a wall at the outlet boundary), sediment mainly deposited along the main flow path, and the influence of paddy ridges was only constrained in its surroundings because of the three-dimensional flow characteristics. The operation of the channel outlets effectively changed the water depth and main flow direction and accordingly influenced the sedimentation distribution on the land surface. Under the shallow-water-depth scenario (open outlet boundary), the ridges on the bed retained more sediment by decreasing the bed-load transport rate. The intersection of the channel and main flow path was blocked by the bed load from the land surface. Hence, setting ridges close to the channel could remarkably relieve sedimentation. The experimental results are helpful for better understanding the mechanism of sediment deposition on paddy fields with complex topography and can provide data for numerical model verification.

Key words: paddy field, sediment deposition, channel, paddy ridge, physical experiment

[1] Graduate School of Engineering, Kyoto University   [2] Disaster Prevention Research Institute, Kyoto University

1. Introduction

Water-related disasters have long been a serious threat to human society and the environment. As a countermeasure, several embankments have been constructed along rivers (Wu, 2011). However, owing to the limited safety level, some triggering mechanisms, such as piping and overtopping, endanger river embankments and even cause failure (Foster et al., 2000; Sills et al., 2008). Moreover, flood inundation caused by embankment breach poses a significant risk to lives and properties. To better understand the embankment failure process and collect related data for the verification of the numerical model, many physical experiments have been conducted. Most of the tests focused on the development and characteristics of embankment breaches (Richards and Reddy, 2007; Xu and Zhang, 2009) and revealed the influence of some key factors, such as the shape and material of the embankment, on the breach process (Schmocker, 2011; Frank, 2016). However, for flood inundation in downstream areas, most laboratory tests have been conducted based on dam breaks (Soares-Frazao and Zech, 2008; Soares-Frazao et al., 2007), instead of embankment breaches.

Another serious but tentatively ignored problem is that a huge amount of sediment is transported and deposited downstream during fluvial inundation (Islam et al., 1994; Takahashi and Nakagawa, 1987). The influence of sedimentation is especially serious for paddy fields. In East Asia, due to monsoons, the climate is characterized by periods of both rain and heat. Hence, summer is very suitable for crop growth, but flood disasters are also likely to happen in this period because of the concentration of annual rainfall. Once an embankment failure occurs, a large quantity of sediment carried by water is transported and deposited on paddy fields, crops are destroyed, and harvests are affected. Moreover, deposition in the channel network disrupts the drainage function and intensi-

fies the impact of inundation (Kawaike et al., 2017). A report of the Ministry of Land, Infrastructure, Transport, and Tourism (MLIT) of Japan shows that, after the dike breach in Japan's Kinu River in 2015, serious sedimentation in paddy fields was difficult to remove and posed a difficult problem to local farmers.

To investigate the sedimentation mechanism on floodplains during fluvial inundation and provide appropriate countermeasures, researchers have conducted a series of laboratory experiments (Takahashi and Nakagawa, 1987; Islam et al., 1994) and numerics (Zech et al., 2008). However, to the best of the authors' knowledge, it is very rare to consider paddy fields as specific targets in investigating sedimentation caused by embankment failures. In paddy fields, two key factors may influence sediment deposition during floods: paddy ridges and the channel network. During inundation, paddy ridges play a role similar to small embankments and divide the farmland into several parts, and the drainage function of the channel network changes the water level and velocity distribution. This paper describes the results of the physical experiments that consider the two factors above. The objectives of this research are as follows:

1) To study the influence of paddy ridges on suspended load deposition during inundation under different scenarios;
2) To investigate the impact of the operation of channel outlets on the sedimentation on the land surface as well as in the channel network;
3) To collect experimental data for numerical model verification in the future.

2. Experimental setup

Fig. 1 shows the plan view of the experimental model that was installed in the Ujigawa Open Laboratory of Disaster Prevention Research Institute (DPRI), Kyoto University. **Fig. 1(a)** and **Fig. 1(b)** shows the layout of paddy ridges and the channel
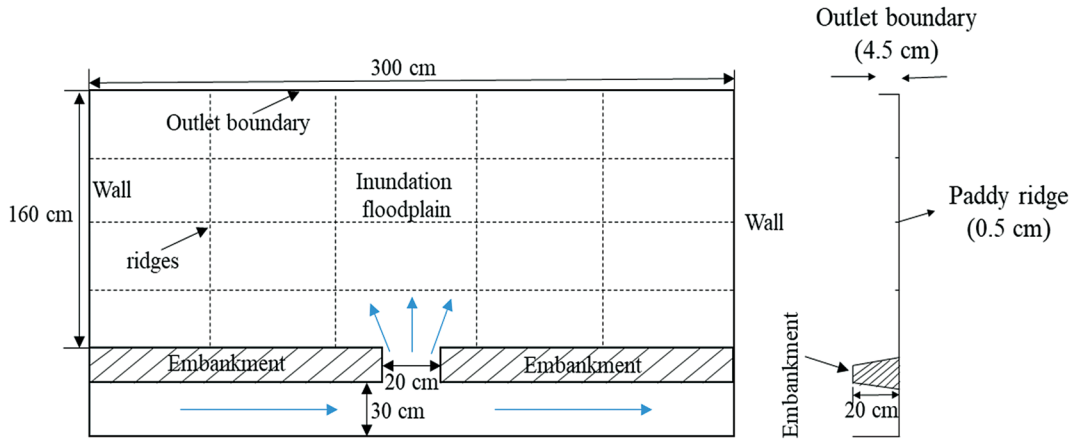
(a) Top and side views of the layout of paddy ridges on the experimental setup
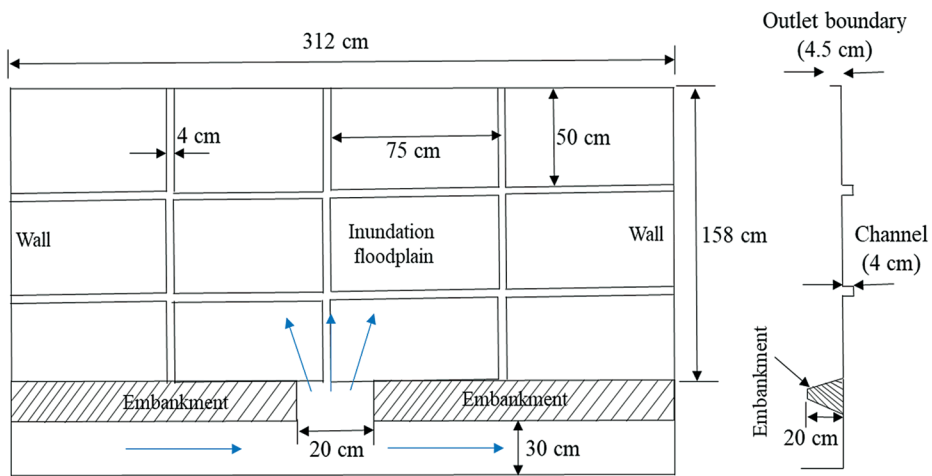
(b) Top and side views of the layout of channel network on the experimental setup

Fig. 1　Layout of ridges and channels on the experimental setup

network on the corresponding experimental setup. The model consists of a flume, embankment, and fixed-bed inundation floodplain. The width of the flume was 30 cm, and its downstream boundary was closed so that all the water flowed into the floodplain through the embankment breach. The slope of the flume was 0, and the flow direction in the flume was parallel to the embankment. The height of the embankment was 15 cm, and a 20-cm-wide breach was set on it to connect the flume and inundation floodplain. The length and width of the floodplain were 300 and 160 cm, respectively. The left and right sides were both closed, and water could only overflow from the outlet boundary. By changing the outlet boundary condition, a series of experimental cases were performed.

Paddy ridges and the channel network are the two key targets of this study. To determine the size

of the ridges, we visited some practical farmlands. The height of paddy ridges varies from 20 cm to 30 cm, and for some main roads, the height is about 50 cm. In addition, the paddy ridges usually have a rectangle cross section and the width is larger than the height. Therefore, to make the scale of the model conform to the practical situation with an approximate length scale ratio of 1:100, pieces of wood with a height of 0.5 cm and a width of 1 cm were set on the inundation floodplain to represent paddy ridges. The size varies from 0.5 m to 5 m in practical farmlands with respect to the irrigation channel network in paddy fields. To simplify the experiment and set the length scale ratio at about 1:100, the width and depth of each channel in the physical model were both set at 4 cm. However, because of the fixed bed, it is impossible to create a channel on the inundation floodplain. Therefore, 12 pieces of wood were placed on the floodplain. The dimensions of the wood were 75 cm long, 50 cm wide, and 4 cm thick, and the distance between each piece of wood was 4 cm. The channel network was accordingly formed, and the width and depth of the channels were the distance between each piece of wood and the thickness of each piece of wood, respectively.

In the experiments, a constant discharge of 2 L/s was given as the inlet discharge. The sediment feeder over the breach supplied uniform sediment into the water at a rate of 1 g/s, and the sediment diameter was 0.01 cm. Table 1 shows the hydraulic condition in the vicinity of the inlet boundary of the case with a lower Froude number and Rouse number. The critical shear velocity is calculated by using the Iwagaki formula (Iwagaki, 1956) and the shear velocity is calculated by Manning's equation:

$$u_* = \sqrt{\frac{gn^2u^2}{h^{1/3}}} \qquad (1)$$

where u_* is the shear velocity, g is the gravity acceleration, h is the water depth, n is the roughness coefficient, and u is the velocity. The shear velocity ratio is 0.93 and the Rouse number is 1.53 in the vicinity of the breach point. From the Rouse number and considering the strong turbulence there, it was generally assumed that suspended load was dominant at the inlet boundary.

Three groups of physical experiments were performed: In the first and second groups, paddy ridges and the channel network were set on the inundation platform respectively to investigate their independent influence on sediment deposition. In the third group, channels and ridges were jointly implemented to clarify their joint effect on sedimentation. In each group, three experimental cases were conducted by changing the conditions of the downstream boundary and channel outlets. Table 2 lists the related information of each case.

3. Results and discussion

3.1 Results of group 1

Fig. 2 shows the deposition results of the three experimental cases. In cases 1 and 2, most of the deposition occurred along the centerline and downstream boundary of the inundation platform. The measured data show that the deposition thickness presented a decreasing trend from the breach of the embankment to the downstream boundary, and the highest thickness was approximately 7 mm in the vicinity of the inlet boundary. Moreover, the

Table 1 Hydraulic parameters near the inlet boundary

Inflow discharge	Mean velocity	Flow depth	Shear velocity	Critical shear velocity	Shear velocity ratio	Fr	Rouse number	Settling velocity	Sediment density
2 L/s	19.2 cm/s	5.2 cm	1.23 cm/s	1.31 cm/s	0.93	0.27	1.53	0.75 cm/s	2.65 g/cm³

Table 2　Information of each experimental case

| Experimental cases		With/without ridges	With/without channels	Outlet boundary height	Duration	Remark
Group 1	Case 1	Without	Without	4.5 cm	45 min	
	Case 2	With	Without	4.5 cm	45 min	
	Case 3	With	Without	0.0 cm	45 min	
Group 2	Case 4	Without	With	4.5 cm	45 min	Outlets 1 to 3 opened
	Case 5	Without	With	4.5 cm	45 min	Outlets 4 to 5 opened
	Case 6	Without	With	4.5 cm	45 min	All outlets closed
Group 3	Case 7	With	With	0.0 cm	45 min	Outlets 1 to 5 opened Ridges are in the paddy center
	Case 8	With	With	0.0 cm	45 min	Outlets 1 to 5 opened Ridges are close to the channels
	Case 9	Without	With	0.0 cm	45 min	Outlets 1 to 5 opened No ridges
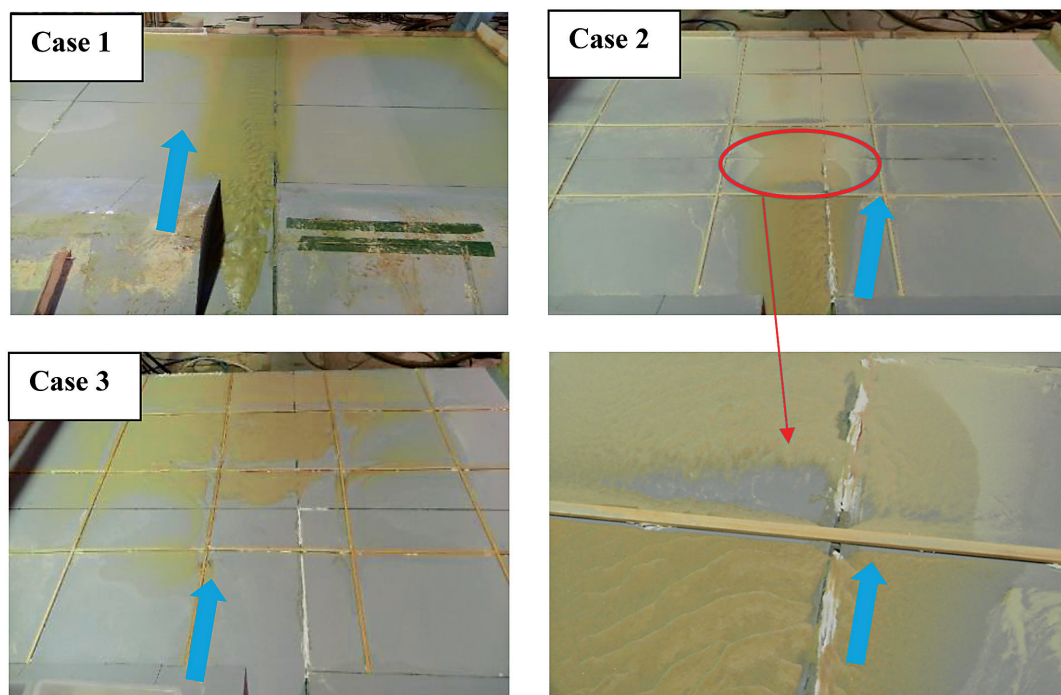
Fig. 2　Experimental results of cases 1, 2, and 3

total quantity of the deposited sediment in the two cases was also similar. The difference between the two cases was only in the area near the ridges. In case 2, the deposition occurred at the backside of the ridges, but at the front side and in the downstream area, no deposition was observed. To determine the reason for this difference, an L-shaped electromagnetic current meter was employed to measure the velocity along the setup centerline under a clear water scenario. The probe was positioned at the desired position inside the water body in different water depths to record the velocity. At each measuring point, the velocity was measured at two layers (1 cm and 3 cm from the bed). The flow velocities at the layers of $z = 1$ cm and $z = 3$ cm were measured in both cases ($z = 1$ cm represents the near-bed velocity and $z = 3$ cm represents the average velocity; water depth h =5.2 cm; and $z \approx 0.6\ h$). **Fig. 3** shows the measured results of the velocity along the centerline. According to the law of vertical velocity distribution, the velocity of the layer $z = 3$ cm should be larger than that of the layer $z = 1$ cm, and the measured results agree well with this. In the figure, the velocity of the layer $z = 3$ cm was almost the same in those of cases 1 and 2, but the bottom velocity of case 2 was obviously lower than that of case 1. In addition, the bottom velocity suddenly decreased when the water flowed through the ridges. Moreover, at the point near the downstream boundary, the value of the bottom velocity was negative in both cases, which means that the water of the bottom layer flows back when it meets a wall. However, this phenomenon was not observed near the ridges. This condition is attributed to the scale effect (the height of the ridges is too small, only 5 mm). However, in practical situations, this phenomenon would be reproduced near ridges. The measurement also recorded the velocity in the vertical direction of each measuring point in the layer $z = 1$ cm (**Fig. 4**). The vertical velocity at the back side of the ridges is negative, which means that the water has a downward velocity after passing the ridges. Based on the measured results, the three-dimensional characteristics of the flow causes the sedimentation difference near the ridges. Owing to the ridges, the water in the bottom layer is obstructed and flows back, so erosion may occur at the front side of the ridges. Furthermore, after the surface layer water flows through the ridges, it has a downward velocity, and then some of the water flows back with sediment, which results in erosion in the downstream area and deposition at the back side of the ridges.

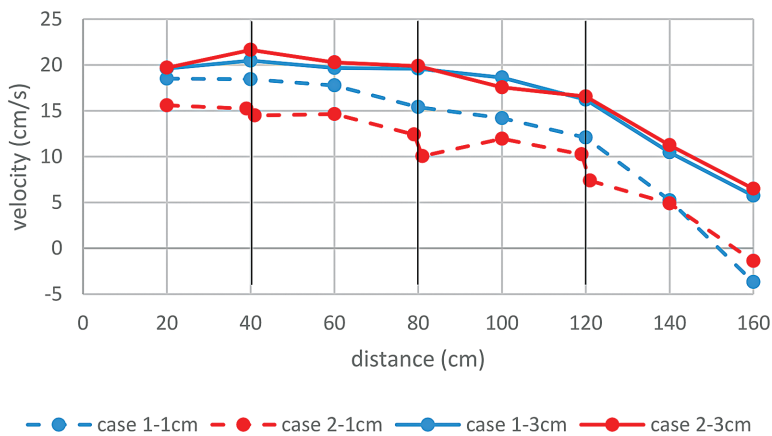The results of case 3 were entirely different

Fig. 3   Velocity distribution along the centerline

from those of the previous two cases. The figure shows that no deposition was observed near the inlet boundary, and the sediment was transported and more uniformly distributed in the downstream area owing to the high shear stress. This phenomenon is more common in practical flood disasters. Some field surveys show that the soil near the breach point is usually eroded and forms a pond (Fujimoto et al., 2019). The figure also shows that some sediment was retained in the upstream area by the paddy ridges.

3. 2 Results of group 2

Fig. 5 shows the experimental results and deposition thickness distribution of each case of group 2. In case 4, channel outlets 1, 2 and 3 were opened during the experiments. The water depth was lower than the height of the wall at the downstream boundary, and all the water could only flow out from the open channel outlets. Because of the high bed shear stress near the inlet boundary, no sediment deposition was found, and most of the sedimentation occurred on the four pieces of wood along the downstream boundary and presented an almost symmetrical distribution. Moreover, the sedimentation in this case was accompanied by a strong sand-wave migration, which means that

bed-load transportation played an important role in this case. In addition, no deposition was observed in the vicinity of the open outlets. This outcome is attributed to the high velocity and turbulence in this area. In case 5, the main flow path clearly deflected to the right side because the two outlets on the right boundary were open. Similar to case 4, most of the sediment was deposited in the downstream area. In the earlier part of the main flow path, the deposition pattern showed the bed-load movement, but, in the latter part, the deposition was almost flat, which means that suspended deposition was the main reason for the sedimentation in this area. In case 6, because all the channel outlets were closed during the experiments, water could only overflow from the downstream boundary. Therefore, the channel network did not have any influence on the sediment deposition on the land surface, and the results presented a similar pattern to that of case 1. The maximum deposition thickness was found in the vicinity of the breach point (approximately 6.5 mm), and deposition occurred along the centerline of the inundation platform. The experimental data also show that the operation of channel outlets can significantly influence the total amount of deposited sediment. The total volumes of deposited sediment in cases 4, 5 and 6 are
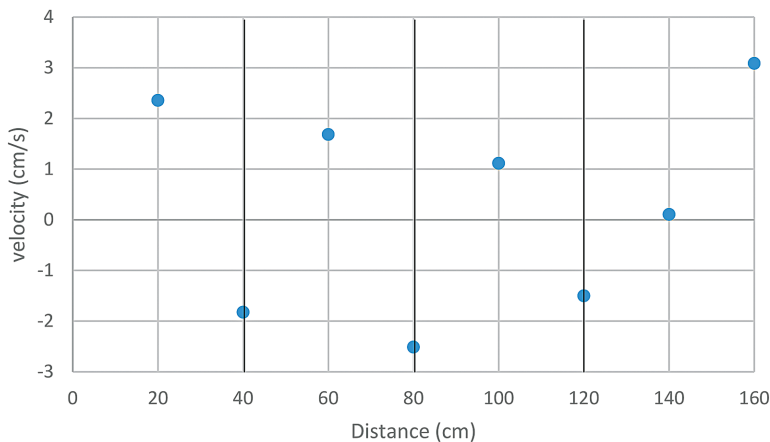

Fig. 4 Vertical velocity distribution along the centerline of case 2
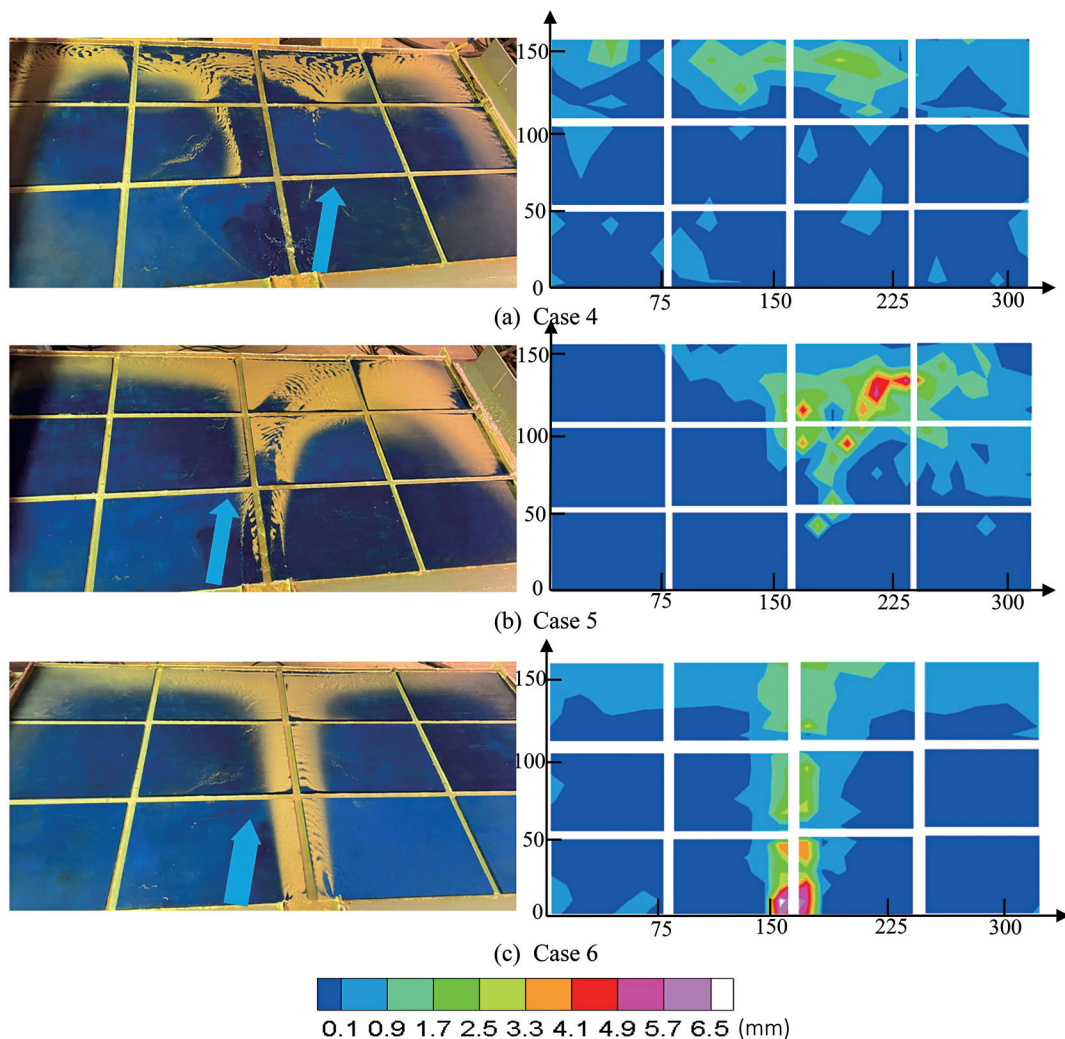
Fig. 5　Experimental results and deposition thickness distribution on land surface of group 2

554.9 cm³, 1301.5 cm³ and 1530.8 cm³, respectively. In case 4, the outlets on the downstream boundary were open, and the water with a higher sediment concentration could be drained out more effectively. Therefore, the bed shear stress was higher and the sediment quantity was less in this case, so the total deposition thickness was obviously lower than that of the other two cases.

Five channels, which were divided into 17 reaches, were set on the platform, and sediment deposition was found in some reaches. Fig. 6 shows the reach number and deposition thickness along the channel network for the three cases. As shown in the figure, the deposition thickness distribution in the channel network is closely related to the main flow path on the land surface. In case 4, continuous sedimentation was formatted from the point 70 cm from the inlet boundary in channel 2, which is much closer than that of the land surface (over 100 cm). By contrast, in channel 4, unlike the continuous sedimentation in channel 2, the deposition was only symmetrically distributed in a part
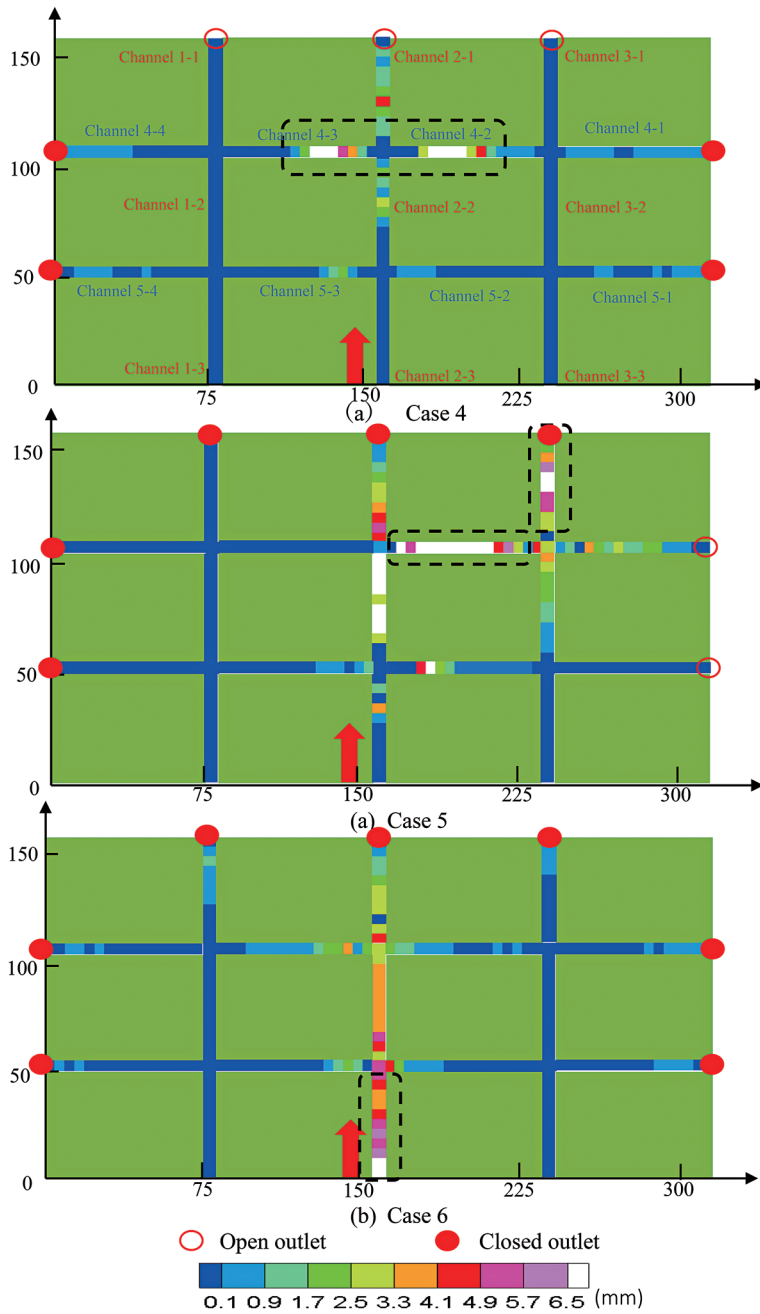
Fig. 6 Sedimentation along the channel network of cases 4, 5 and 6

of reaches 4-2 and 4-3. In addition, the deposition here presented a slope along the cross section of the channel. At the upstream side, the highest thickness was over 1 cm, much higher than that in channel 2 (approximately 6 mm) and on the land surface (approximately 2.7 mm), but the deposition thickness at the downstream side was only less than 5 mm. The bed load was the main reason

for the blockage. A similar phenomenon was also observed in case 5, but because the main flow path deflected to the right side, sedimentation did not occur in reach 4-3, but in reaches 4-2 and 3-1. Moreover, because the outlets of channel 2 were closed, the sedimentation thickness in this channel was much higher than that in case 4. In case 6, the location of deposition in the channels agrees better with the land surface than cases 4 and 5 because suspended load was the main reason for sedimentation in this case. However, owing to the higher water depth, the deposition thickness in the channels was obviously higher than that on the adjacent surface area.

3. 3   Results of group 3

Previous experiments found that most of the sediment was deposited only on the specific area that the main flow passed. Therefore, to reduce the measurement time, the width of the inundation platform was decreased from 300 to 160 cm. By changing the location of the ridges, three cases were performed to investigate the sedimentation on paddy fields. **Fig. 7** shows the experimental results and the deposition thickness distribution. Unlike cases 1 and 2, the influence of ridges was only limited to the adjacent area less than 10 cm, and the sedimentation results of the three cases were quite different. In case 7, two rectangular areas upstream of the ridges retained most of the sediment (shown in **Fig. 7(a)**), and most of the deposition in case 8 was formatted along the ridges. In addition, paddy ridges significantly influenced the total amount of sedimentation. **Fig. 8** depicts the quantity of sediment deposited on the land surface. Compared with cases 7 and 8, less sediment was retained on the bed by paddy ridges in case 9. The different layout of ridges could only change the deposition distribution, but not the total amount of sediment. This finding is attributed to the very small water depth (less than 1 cm) and

relatively larger bed shear stress. Because of the high shear stress, once the suspended load was deposited, it moved from the bed to the channels in the form of bed load and was then drained out, but the existence of ridges could decrease the bed load transport rate and retain more sediment on the land surface.

In this group of experiments, only the channel perpendicular to the main flow direction showed significant sedimentation. In the fluvial inundation in Kinu River in 2015, serious sedimentation was also found in the channels that were on the main flow path. **Fig. 9** shows the deposition thickness along the channel. The figure shows that the setting ridges at the upstream side could effectively alleviate sedimentation in the channel network. The maximum deposition thicknesses of cases 7, 8, and 9 were 15.96, 7.56, and 12.19 mm, respectively.

4. Conclusions

A series of physical experiments were conducted to investigate the suspended load deposition on the paddy field caused by embankment failures by considering the influence of paddy ridges and the channel network. For the higher-water-depth cases, the sediment was mainly deposited along the main flow path, and the maximum deposition thickness was found in the vicinity of the inlet boundary. Under this scenario, setting paddy ridges did not change the total amount of sedimentation on the bed, and its influence was limited to the surrounding area because of the three-dimensional flow characteristics. However, for the shallow-water-depth cases, the sediment was carried by water and more uniformly deposited in the downstream area. The ridges could effectively decrease the bed-load transport rate, which resulted in a large amount of sediment deposited in the upstream area and along the ridge, and the maximum deposition thickness was found at the front side of the ridge. In the experiments, the op-
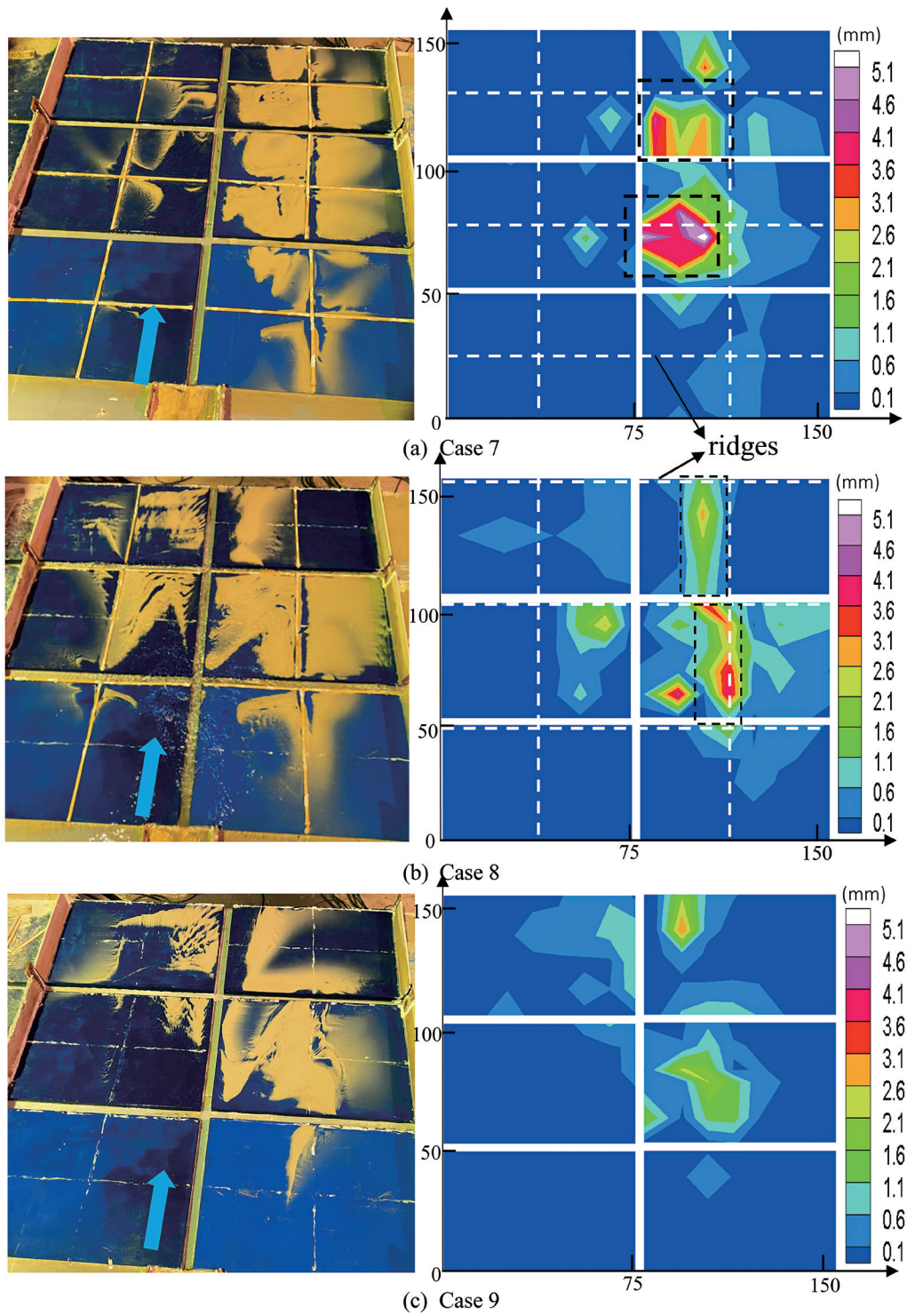
(a) Case 7

(b) Case 8

(c) Case 9

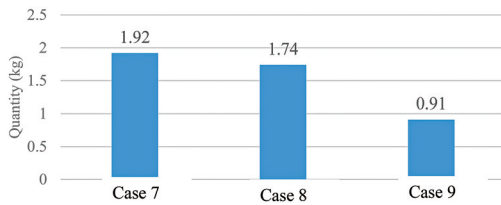Fig. 7　Experimental results and deposition thickness distribution of group 3

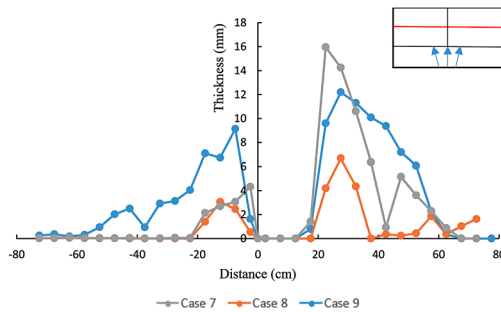**Fig. 8** The quantity of deposition on the bed of cases 7, 8, and 9

Fig. 9 Deposition thickness along the channel

eration of the channel outlets significantly changed the water depth and flow velocity, and the main flow direction clearly deflected to the open outlets. The results show that opening the channel outlets could drain out the sediment more effectively and alleviate sedimentation on the land surface. However, the channel can also be blocked by sediment. The maximum deposition thickness in the channel occurred at the point where the main flow passed, which was mainly caused by the bed load from the land surface. By setting ridges on the bed, the ridges retained more sediment on the bed. Conversely, setting ridges at the channel's upstream side would be helpful in decreasing the sedimentation in the channel network. However, some factors were not considered in this study. For example, the vegetation in paddy fields may have significant influence on the flow propagation and sediment deposition. Further physical experiments and numerical simulations considering different conditions are necessary to better understand the mechanism.

References

Foster, M., Fell, R., and Spannagle, M (2000): The statistics of embankment dam failures and accidents, *Canadian Geotechnical Journal*, Vol. 37, No. 5, pp. 1000-1024.

Frank, P. J. (2016): Hydraulics of spatial dike breaches, PhD thesis, Swiss Federal Institute of Technology Zurich, Switzerland.

Fujimoto S., Koyama T., and Yamada M. (2019): Preliminary report on flooding and building damage surveys on the Naka River due to Typhoon No. 19 in 2019 (in Japanese).

Islam, Md. Z., Okubo, K., Muramoto, Y., and Morikawa, H. (1994): Experimental study on sedimentation over the floodplain due to river embankment failure, *Bulletin of the Disaster Prevention Research Institute*, Kyoto University, Vol. 44, Part 2, No. 380, pp. 69-92.

Iwagaki Y. (1956): Fundamental study on critical tractive force. *JSCE Trans.,* Vol. 41, pp. 1-21.

Kawaike, K., Hashimoto, M., and Nakagawa, H. (2017): Numerical simulation of flood inundation and sedimentation considering the effects of paddy field, *Proceedings of the 37th IAHR World Congress*, Kuala Lumpur, Malaysia.

Richards, K. and Reddy, K. (2007): Critical appraisal of piping phenomena in earth dams, *Bulletin of Engineering Geology and the Environment*, Vol. 66, No. 4, pp. 381-402.

Schmocker, L. (2011): Hydraulics of dike breaching, PhD thesis, Swiss Federal Institute of Technology Zurich, Switzerland.

Sills, G. L., Vroman, N. D., Wahl, R. E., and Schwanz, N. T (2008): Overview of New Orleans levee failures: Lessons learned and their impact on national levee design and assessment, *Journal of Geotechnical and Geoenvironmental Engineering*, Vol. 134, No. 5, pp. 556-565.

Soares-Frazao, S., Le Grelle, N., Spinewine, B., and Zech, Y. (2007): Dam-break induced morphological changes in a channel with uniform sediments: Measurements by a laser-sheet imaging technique, *Journal of Hydraulic Research*, IAHR, Vol. 45, No. 1, pp. 87-95.

Soares-Frazao, S. and Zech, Y. (2008): Dam-break flow through an idealized city, Journal of Hydraulic Research, IAHR, Vol. 46, No. 5, pp. 648-658.

Takahashi, T. and Nakagawa, H. (1987): Suspended sediment deposition in flood zone due to river bank breach, *Annals of the Disaster Prevention Research Institute*, Kyoto University, No. 30 B-2, pp. 597–609.

Wu, W. M. (2007): Earthen embankment breaching, *J. Hydraulic. Engineering*, ASCE, Vol. 137, No. 12, pp. 1549–1564.

Xu, Y. and Zhang, L. M. (2009): Breaching parameters for earth and rock-fill dams, *Journal of Geotechni-cal and Geoenvironmental Engineering*, Vol. 135, No. 12, pp. 1957–1969.

Zech, Y., Soares-Frazao, S., Spinewine, B., and Le Grelle, N. (2008): Dam-break induced sediment movement: Experimental approaches and numerical modeling, Journal of Hydraulic Research, IAHR, Vol. 46, No. 2, pp. 176–190.

要　　旨

　本研究では，水田における畦畔と灌漑水路が洪水氾濫時の土砂堆積に及ぼす影響を評価するため，室内実験を行った。堤防決壊条件を模擬するため，流入境界において一定の流量と土砂を供給した。下流端境界と水路の流出条件を変更することで，大まかに 3 種類の実験を行った。その結果，氾濫水位が高い条件では，主に氾濫流の主流方向沿いに土砂が堆積し，畦畔の影響はその周辺に限定された。さらに，水路の流出条件が変われば水深と氾濫流の主流方向が大きく変更し，それに応じて氾濫原での土砂堆積分布も変化した。氾濫水位が低い条件では，掃流砂量が減少するためより多くの土砂が畦畔の周辺に堆積した。水路やその合流点は氾濫原からの掃流砂が堆積するが，氾濫流の上流側に畦畔を設置することで水路への土砂の堆積を防止することができる。